Ground-state vortex lattice structures in *d*-wave superconductors

Sudhansu S. Mandal*,† and T. V. Ramakrishnan*
Centre for Condensed Matter Theory, Department of Physics, Indian Institute of Science, Bangalore 560 012, India
(Received 30 November 2001; published 25 April 2002)

We show in a realistic $d_{x^2-y^2}$ symmetry gap model for a cuprate superconductor that the clean vortex lattice has discontinuous structural transitions (at and near $T=0$), as a function of the magnetic field B along the c axis. The transitions arise from the singular nonlocal and anisotropic susceptibility of the $d_{x^2-y^2}$ superconductor to the perturbation caused by supercurrents associated with vortices. The susceptibility, due to virtual Dirac quasiparticle-hole excitation, is calculated carefully and leads to a ground-state transition for the triangular lattice from an orientation along one of the crystal axis to one at 45° to them, i.e., along the gap zero direction. The field scale is seen to be 5 T $\sim(\Delta_0/ta)^2\Phi_0$, where Δ_0 is the gap maximum, t is the nearest-neighbor hopping, a is the lattice constant, and Φ_0 is the flux quantum. At much higher fields ($\sim$28 T) there is a discontinuous transition to a centered square structure. The source of the differences from existing calculations and experimental observability are discussed, the latter especially in view of the very small (a few degrees K per vortex) differences in the ground-state energy.

DOI: 10.1103/PhysRevB.65.184513 PACS number(s): 74.60.Ge

I. INTRODUCTION

An external magnetic field enters a (type-II) superconductor as a collection of quantized magnetic flux tubes. The flux tubes with associated supercurrent vortices form a triangular lattice[1] as is seen in conventional superconductors.[2,3] Deviations from this structure are of considerable interest. In conventional superconductors, the observed deviations have been attributed to the anisotropy of the underlying one electron energy spectrum. In heavy-fermion and high-T_c superconductors, an additional and potentially very interesting reason is the existence of an unconventional superconducting order parameter, with gaps which have nodes and change sign. Indeed there is experimental evidence in the heavy-fermion systems,[4] in the exotic superconductor $SrRuO_4$,[5] and in cuprate superconductors[6,7] that the vortex lattice is not triangular (for some field and temperature regimes). Recently, measurements of small-angle neutron diffraction from untwinned $YBa_2Cu_3O_{7-\delta}$ single crystals shows a very well-formed triangular lattice that undergoes an orientational transition from along the a axis to along the b axis for a 3 T magnetic field at 33° to the c axis.[8] The reasons for possible nontriangular structure as well as for the structural transition are not fully established and are the subject of considerable theoretical work.[9–13] In high-T_c superconductors, entropic effects, abetted by a high transition temperature as well as a weak interlayer coupling, play an important role, and the classical statistical mechanics of interacting, meandering flux lines, of the vortex fluid phase, and the solid fluid transition has developed into a major theoretical and experimental subfield.[14]

In this paper, we focus on the nature of the flux lattice at temperatures well below the superconducting transition, where vortex configurational entropy effects mentioned above are negligible. The ground-state structures and structural transition then directly reflect the electronic peculiarities of the superconductor and, thus, probe the latter. For cuprate superconductors, a number of measurements show that the superconducting gap $\Delta_{\mathbf{k}}$ has nodes,[15] has a magnitude with a $(\Delta_0/2)|\cos k_x a-\cos k_y a|$ dependence on the two-dimensional wave vector $\mathbf{k}$ across the Fermi surface,[16] and that transport lifetimes of quasiparticles are long[17] for $T \ll T_c$. Thus one can assume well-defined low-energy, nodal quasiparticles, with an experimentally determined one-electron dispersion $\epsilon_{\mathbf{k}}$ (Ref. 18) and gap function $\Delta_{\mathbf{k}}$.[16] The question of interest is the effect of the zero-gap, anisotropic Dirac-like linear quasiparticle excitation spectrum on the interaction between vortices and, thus, on vortex lattice structure. There is considerable evidence, e.g., from magnetic-field-dependent electronic specific heat,[19] electronic thermal conductivity,[20] and superfluid density[21] measurements that an external magnetic field going in as vortices has a strong effect on electronic states, changing their density and lifetime. The relevant issue here is somewhat the reverse: namely, the effect of the quasiparticles on the interaction between vortices. The order parameter phase associated with the vortex and the related magnetic vector potential together constitute the superfluid velocity field $\mathbf{v}_s(\mathbf{r})[=\Sigma_l \mathbf{v}_s(\mathbf{r}-\mathbf{R}_l)]$ where the vortices are located at points $\mathbf{R}_l$. The extra superfluid kinetic energy, being quadratic in v_s, clearly has a part that depends on two vortex coordinates and is thus structure sensitive. In addition to this ''diamagnetic'' term, which is the additional kinetic energy of the rigidly moving superfluid and which is minimized for a triangular lattice,[1] there is another ''paramagnetic'' term due to the perturbation of quasiparticles by the superfluid current via the term $\mathbf{k}\cdot\mathbf{v}_s$. This causes virtual particle hole excitations; two vortices interact via the exchange of quasiparticle-quasihole pairs. This polarization term depends on the quasiparticle excitation spectrum. In a clean *s*-wave superconductor, the process leads to an additional isotropic interaction between vortices of order (H/H_{c_2}) relative to the diamagnetic term. However, in a *d*-wave superconductor where the excitation gap vanishes along some (nodal) directions, one expects the nonlocal polarizability to be larger as well as anisotropic; this gives rise to an interaction between vortices which depends on the orientation of the line joining them with the respect to crystal-

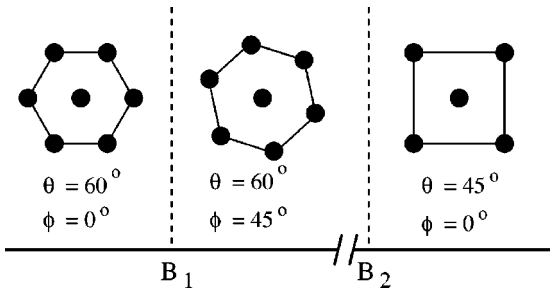

FIG. 1. Phase diagram for the structure of the vortex lattice. The position of the vortices are denoted by solid circles. B_1 and B_2 are the fields at which the structural transitions take place as described in the text. The structures are shown diagrammatically.

ine axes and consequently, can be the cause of novel long-range positional order.

The ground-state energy arising from quasiparticle-hole-mediated interaction between vortices depends linearly on the nonlocal current susceptibility $\chi^{\rm p}_{\alpha\beta}(\mathbf{q})$, for wave vectors $\mathbf{q}$ equal to the reciprocal lattice vectors $\mathbf{G}$ of the vortex lattice. Because the gap as well as the density of quasiparticle states vanishes linearly near the node, $\chi^{\rm p}_{\alpha\beta}(\mathbf{q})$ is proportional to $|q_x|$ or $|q_y|$ for small q. This nonanalytic behavior, noticed first by Kosztin and Leggett,[22] has also been discussed by Franz *et al.*[12] who were the first to analyze microscopically its effect, as well as of the anisotropy in $\chi^{\rm p}_{\alpha\beta}$, on vortex lattice structure at $T=0$. These authors found a rich phase diagram in the field-temperature plane, with a centered rectangular lattice at $T=0$ whose inner angle varies *continuously* as a function of field, as well as a sudden orientational transition at higher temperatures and a transition to a centered square lattice for very high fields and low T. In obtaining these results, Franz *et al.* made a ''local'' approximation for the gap function, i.e., assumed $\Delta_{\mathbf{k}}=\Delta_{\mathbf{k}+\mathbf{G}}$, and more importantly they assumed a momentum-independent quasiparticle current which leads to a response function $\chi^{\rm p}_{xx}(\mathbf{G})=\chi^{\rm p}_{yy}(\mathbf{G})$. The anisotropy then enters only through $\chi^{\rm p}_{xy}(\mathbf{G})$. We carry out here a more detailed and realistic calculation of the nonlocal susceptibility, considering the strong $\mathbf{k}$ dependence of the gap function $\Delta_{\mathbf{k}}$ and quasiparticle current $\mathbf{j}_{\mathbf{k}}$ properly, and using a realistic one-electron dispersion. The diagonal terms $\chi^{\rm p}_{xx}$ and $\chi^{\rm p}_{yy}$ are unequal and large, and this anisotropy is seen to be the underlying cause of the transition discussed below. The contibution of the off-diagonal susceptitiblity $\chi^{\rm p}_{xy}$ is smaller than that of the diagonal susceptibilities. Our results for structural stability (at $T=0$) are therefore quite different from those of Franz *et al.*[12,13]

Confining ourselves to $T=0$, we find, as summarized in a phase diagram (see Fig. 1), that the stable lattice at low fields is triangular. At about 5 T (for the parameters chosen) the orientation of the smallest $\mathbf{G}$ vector changes from being along one of the axes to being along the order parameter node direction, because the system is most susceptible to excitations with the wave vector along the node. We have analyzed the driving force for this transition, both analytically and numerically, and find that it arises from a subtle balance between the term linear in $|\mathbf{G}|$ and the quadratic term, which are slightly different for the two orientations.

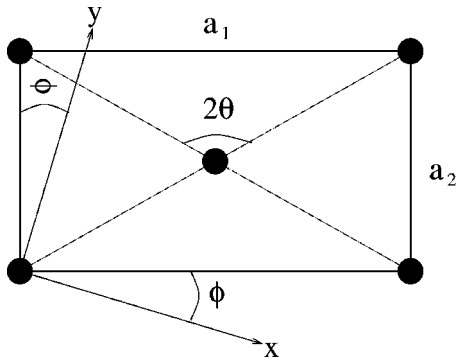

FIG. 2. A typical centered rectangular vortex lattice. Solid circles represent the position of the vortices in the lattice. The aspect ratio of the lattice is given by $a_1/a_2=\tan\theta$. The angle ϕ represents the inclination of the lattice with respect to the crystal axis which is parallel to the x and y directions.

The field scale for the transition is approximately given by the condition $(taG/\Delta_0)\sim 1$ which is natural on dimensional grounds. The Fermi velocity is ta and the energy scale associated with the superflow $(\boldsymbol{\nabla}\theta)$ with Fourier component G is therefore taG. The polarizability or susceptibility has an energy scale $(1/\Delta_0)$ where Δ_0 is the gap magnitude which sets the scale for quasiparticle excitation energies. Thus the dimensionless susceptibility of interest is (taG/Δ_0). For realistic parameters t,a, and Δ_0 this translates $[(taG_c/\Delta_0)\simeq 0.37]$ to a field scale of 5.2 T.

We find that the node-oriented triangular lattice is stable until about 28 T, whereupon a discontinuous transition to a centered square lattice takes place. This structure, which is orientationally commensurate with the symmetry of the quasiparticle dispersion, is probably the most stable $T=0$ phase when electronic commensurate effects dominate. However, the calculated field scale is large enough that the London approximation used, valid for $H\ll H_{c_2}$, is not reliable, because vortex core effects cannot be neglected at these high fields.

In the next section (Sec. II), we describe the model and the theoretical approach used. The tight-binding quasiparticle Hamiltonian is decomposed into an unperturbed part H_0 and a term H_I due to the quasiparticle vortex interaction. The free energy or the ground-state energy can be obtained as a power series in H_I or equivalently the density of vortices. For low vortex densities $(H\ll H_{c_2})$ the leading or n_v^2 term is sufficient and describes quasiparticle-hole-mediated vortex interactions, in addition to the bare superfluid kinetic energy. We discuss the former carefully in terms of the nonlocal, anisotropic current susceptibility $\chi^{\rm p}_{\alpha\beta}(\mathbf{q})$ since the energy can be expressed as a reciprocal lattice vector sum over $\chi^{\rm p}_{\alpha\beta}(\mathbf{G})$. We obtain $\chi^{\rm p}_{\alpha\beta}(\mathbf{q})$ semianalytically for small q at $T=0$, as well as numerically (Sec. III).

The calculations for different two-dimensional structures are discussed in Sec. III. For a given magnetic field B the most general centered rectangular lattice $[a_1,a_2]$ can be described in terms of an angle θ related to the aspect ratio (a_1/a_2) as $\tan\theta=a_1/a_2$ and an orientation ϕ with respect to crystal axes (Fig. 2). We compute the ground-state energy

as a function of these two variables for different magnetic fields. The basic vortex-related electronic energy parameters are the following. The vortex has three energy scales: namely, the diamagnetic single-vortex energy, of order 3450 K per vortex; the vortex interaction energy, the diamagnetic part of which has a value ~ 1440 K (for nearest-neighbor vortices); and the paramagnetic interaction term which is about 350 K at 5 T field. The last and the smallest term is structure sensitive and is of interest here. The ground state is analyzed as a function of θ, ϕ for several field values in Sec. III. It turns out that the structure-sensitive part of the last (paramagnetic vortex interaction) term is extremely small, of order a few degrees per vortex. This has obvious implications for the observability of the transition, because the structural changes predicted and the clean limit anisotropies obtained can be easily overwhelmed by effects of disorder, e.g., vortex pinning and the muting of the paramagnetic susceptibility anisotropy, and nonanalyticity by disorder. However, the size of the structure sensitive terms is larger, the greater the (v_F/v_Δ) ratio or anisotropy. One can thus imagine situations where this effect is quite large.

In the concluding section (Sec. IV) we briefly discuss thermal effects, the consequences of the predicted transition and their observability, the reason for which our result differs from earlier results, and the experimentally observed structural transitions.

II. THEORY

A. Model

We consider a two-dimensional lattice model with nearest-neighbor and next-nearest-neighbor hopping for a CuO_2 plane of high-T_c superconductors. The (mean-field) Hamiltonian in this model is given by

$$H_0 = -t\sum_{\langle ij\rangle\sigma}(c^\dagger_{i\sigma}c_{j\sigma}+\text{H.c.})+t'\sum_{\langle\langle ij\rangle\rangle\sigma}(c^\dagger_{i\sigma}c_{j\sigma}+\text{H.c.}) + \sum_{\langle ij\rangle}(\Delta_{ij}c^\dagger_{i\uparrow}c^\dagger_{j\downarrow}+\text{H.c.})-\mu\sum_i c^\dagger_{i\sigma}c_{i\sigma}, \tag{1}$$

where t and t' are nearest-neighbor and next-nearest-neighbor hopping integrals, respectively. This corresponds for appropriate choices of t and t' to an open Fermi surface which is observed in angle-resolved photoemission experiments. The pair amplitude Δ_{ij} is considered to be $d_{x^2-y^2}$-wave like, i.e., $\Delta_{i,i\pm a\hat{x}}=-\Delta_{i,i\pm a\hat{y}}$, where a is the lattice constant in a square lattice and μ is the chemical potential.

When we apply a magnetic field beyond the lower critical field H_{c_1} in high-T_c superconductors, the magnetic field goes into the system in the form of vortices. The magnetic induction is screened over a length λ, the penetration depth. The pair amplitude acquires a phase $\Delta_{ij}\to\Delta_{ij}\exp[-i\theta_{ij}]$, where θ_{ij} is the sum of polar angles of all the vortices measured with respect to a particular axis, for the center of mass of the pair ij. We write θ_{ij} as $(\theta_i+\theta_j)/2$ (as an average of the angles of individual coordinates of the Cooper pairs), which is consistent up to $\mathcal{O}(1/k_F\xi)^2$, where k_F is the Fermi momentum and ξ is the superconductive coherence length. The pair amplitude (order parameter magnitude) vanishes at the center of the core of a vortex, and over a distance ξ it acquires its uniform value. For a collection of vortices with $H\ll H_{c_2}$, i.e., with intervortex spacing $\gg\xi$ or the London limit, we assume the order parameter magnitude to be uniform throughout the superconductor (there are δ function sources of phase rotation at the locations of vortices). There is a vector potential $\mathbf{A}$ such that $\boldsymbol{\nabla}\times\mathbf{A}(\mathbf{r})=B(\mathbf{r})$ where $B(\mathbf{r})$ is the local magnetic induction, along the c axis. Its effect in this model is to change the hopping integrals to

$$(t,t')\to(t,t')\exp\left[i(e/\hbar c)\int_{\mathbf{r}_i}^{\mathbf{r}_j}\mathbf{A}\cdot d\mathbf{l}\right] \tag{2}$$

for hopping from site j to site i. We then make a gauge transformation $c_{i\sigma}\to c_{i\sigma}e^{-i\theta_i/2}$. We thus obtain the Hamiltonian as

$$\begin{aligned}H=&-t\sum_{\langle ij\rangle\sigma}\left\{c^\dagger_{i\sigma}c_{j\sigma}\exp\left[i(\theta_i-\theta_j)/2+i(e/\hbar c)\int_{\mathbf{r}_i}^{\mathbf{r}_j}\mathbf{A}\cdot d\mathbf{l}\right]\right.\\&\left.+\text{H.c.}\right\}+\sum_{\langle ij\rangle\sigma}(\Delta_{ij}c^\dagger_{i\uparrow}c^\dagger_{j\downarrow}+\text{H.c.})\\&+t'\sum_{\langle\langle ij\rangle\rangle}\left\{c^\dagger_{i\sigma}c_{j\sigma}\exp\left[i(\theta_i-\theta_j)/2+i(e/\hbar c)\int_{\mathbf{r}_i}^{\mathbf{r}_j}\mathbf{A}\cdot d\mathbf{l}\right]\right.\\&\left.+\text{H.c.}\right\}-\mu\sum_i c^\dagger_{i\sigma}c_{i\sigma}.\end{aligned} \tag{3}$$

The phase difference between two nearest- or next-nearest-neighbor sites can be expressed as

$$\begin{aligned}\frac{1}{2}(\theta_i-\theta_j)+(e/\hbar c)\int_{\mathbf{r}_i}^{\mathbf{r}_j}\mathbf{A}\cdot d\mathbf{l}&\simeq(\mathbf{r}_i-\mathbf{r}_j)\cdot\left(\frac{1}{2}\boldsymbol{\nabla}_i\theta-(e/\hbar c)\mathbf{A}_i\right)\\&\equiv(m/\hbar)(\mathbf{r}_i-\mathbf{r}_j)\cdot\mathbf{v}_s(\mathbf{r}_i).\end{aligned} \tag{4}$$

Here the superfluid velocity

$$\mathbf{v}_s(\mathbf{r})=\frac{1}{m}\left[\frac{\hbar}{2}\nabla\theta-\frac{e}{c}\mathbf{A}(\mathbf{r})\right] \tag{5}$$

for a single vortex and for a collection of vortices, $\mathbf{v}_s(\mathbf{r})=\Sigma_l\mathbf{v}_s(\mathbf{r}-\mathbf{R}_l)$ (where the vortices are located at $\mathbf{R}_l$. We then assume that the phase difference between two neighboring lattice sites is very small (which is certainly true in the London limit) so that we expand exponentials in Eq. (3) up to quadratic terms.

Using Eqs. (5) and (4) in Eq. (3) for H and expanding up to quadratic order in the small quantity $\mathbf{v}_s(\mathbf{r})$ we have

$$H=H_0+H_I+H_{II}, \tag{6}$$

where the free Hamiltonian

$$H_0=\sum_{\mathbf{k},\sigma}\xi_{\mathbf{k}}c^\dagger_{\mathbf{k}\sigma}c_{\mathbf{k}\sigma}+\sum_{\mathbf{k}}[\Delta_{\mathbf{k}}c^\dagger_{\mathbf{k}\uparrow}c^\dagger_{-\mathbf{k}\downarrow}+\text{H.c.}], \tag{7}$$

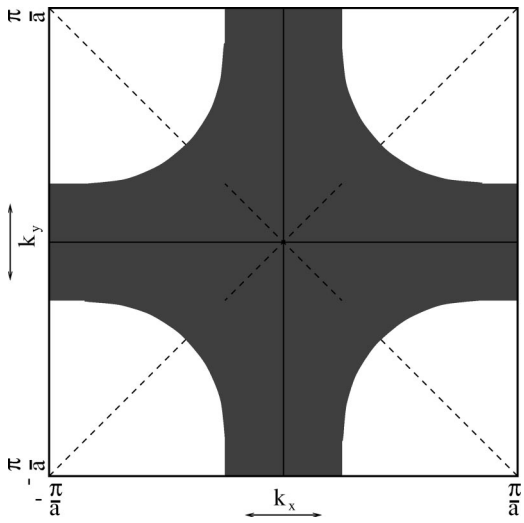

FIG. 3. A typical open Fermi surface for high-T_c compounds which can be parametrized by a t-t' model. The shaded region denotes the occupied states with concentration $1-x$, where x is the doping concentration. The superconducting state is gapless along the diagonals of the Brillioun zone

with $\xi_{\mathbf{k}}=-2t[\cos(k_x a)+\cos(k_y a)]+4t'\cos(k_x a)\cos(k_y a)-\mu$ and $\Delta_{\mathbf{k}}=(\Delta_0/2)[\cos(k_x a)-\cos(k_y a)]$, Δ_0 being the maximum quasiparticle excitation gap. Here $\mathbf{k}$ lies in the first atomic Briliouin zone, (BZ) i.e., $-\pi/a\leqslant(k_x,k_y)\leqslant\pi/a$. A typical structure of the Fermi surface is shown in Fig. 3. Gapless quasiparticle excitations exist along $k_x=\pm k_y$ directions as noted in the figure. The interaction term (first order in v_s) can now be expressed as

$$\begin{aligned}H_I=&2(at/\hbar)\sum_{\mathbf{k}}\sum_{\mathbf{G}>0}[c^{\dagger}_{\mathbf{k}\sigma}c_{\mathbf{k}+\mathbf{G}\sigma}-c^{\dagger}_{\mathbf{k}+\mathbf{G}\sigma}c_{\mathbf{k}\sigma}]\\&\times[mv_s^x(\mathbf{G})\sin(k_x a)+mv_s^y(\mathbf{G})\sin(k_y a)]\\&-4(at'/\hbar)\sum_{\mathbf{k}}\sum_{\mathbf{G}>0}[c^{\dagger}_{\mathbf{k}\sigma}c_{\mathbf{k}+\mathbf{G}\sigma}-c^{\dagger}_{\mathbf{k}+\mathbf{G}\sigma}c_{\mathbf{k}\sigma}]\\&\times[mv_s^x(\mathbf{G})\sin(k_x a)\cos(k_y a)+mv_s^y(\mathbf{G})\sin(k_y a)\\&\times\cos(k_x a)]\equiv\sum_{\mathbf{k}\boldsymbol{\sigma}}\sum_{G>0}V_{\mathbf{k},\mathbf{G}}[c^{\dagger}_{\mathbf{k}\sigma}c_{\mathbf{k}+\mathbf{G}\sigma}-c^{\dagger}_{\mathbf{k}+\mathbf{G}\sigma}c_{\mathbf{k}\sigma}].\end{aligned}\tag{8}$$

Here $V_{\mathbf{k},\mathbf{G}}$ is purely imaginary. The term H_{II} is quadratic in v_s and contributes to the free energy as a diamagnetic term. It is given by

$$H_{II}=2N_s^0(t-t')(a^2/\hbar^2)\sum_{\mathbf{G}}mv_s^{\alpha}(\mathbf{G})mv_s^{\alpha}(-\mathbf{G}),\tag{9}$$

with N_s^0 being the number of superfluid carriers, and α refers to Cartesian variables x and y. Paramekanti *et al.*[23] have recently shown that the quantum phase fluctuation of the order parameter reduces the superfluid density considerably. We thus reexpress the term H_{II} phenomenologically in terms of the measured λ as

$$H_{II}=\frac{dA}{2\lambda^2}\left(\frac{c^2}{4\pi e^2}\right)\sum_{\mathbf{G}}mv_s^{\alpha}(\mathbf{G})mv_s^{\alpha}(-\mathbf{G}),\tag{10}$$

where d is the mean interlayer separation of weakly coupled superconducting layers and A is the area of the system.

B. Free energy

We now calculate the free energy as a power series in $\mathbf{v}_s(\mathbf{r})$ or equivalently the vortex density. The diamagnetic or Ginzburg-Landau term, of first order in H_{II}, is the largest, and the structure sensitive part of it is known to be minimized for a triangular lattice (1). The energy does not depend on its orientation with respect to the crystal lattice. We are interested here additionally in the paramagnetic term, of second order in H_I. Including this and the magnetic field energy contribution, the free energy to second order in vortex density is given (per unit length along the c axis) by

$$\begin{aligned}\Delta\Omega=&\frac{1}{2Ad\hbar^2}\sum_{\mathbf{G}}mv_s^{\alpha}(\mathbf{G})[\chi^d\delta_{\alpha\beta}-\chi^{\mathrm{p}}_{\alpha\beta}(\mathbf{G})]mv_s^{\beta}(-\mathbf{G})\\&+\frac{1}{8\pi A}\sum_{\mathbf{G}}B_{\mathbf{G}}B_{-\mathbf{G}},\end{aligned}\tag{11}$$

where $\mathbf{G}$ is the reciprocal vector of the vortex lattice. The individual vortex energy is not included here, as it is not relevant for the question of vortex lattice structure. $\chi^d=(c^2\hbar^2 d/4\pi e^2\lambda^2)$ is the diamagnetic term arising from the term H_{II} [Eq. (10)] to first order, and $\chi^{\mathrm{p}}_{\alpha\beta}(\mathbf{G})$ is the paramagnetic current susceptibility due to the second-order contribution from H_I. Higher-order contributions are neglected since the expansion parameter is (n_v/n) where n_v is the vortex density and n is the electron density. This ratio is obviously much smaller than 1.

The paramagnetic susceptibility $\chi^{\mathrm{p}}_{\alpha\beta}(\mathbf{q})$ is expressed as

$$\chi^{\mathrm{p}}_{\alpha\beta}(\mathbf{q})=\frac{1}{(2\pi)^2}\int_{-\pi/a}^{\pi/a}dk_x\int_{-\pi/a}^{\pi/a}dk_y\gamma_{\alpha\beta}(\mathbf{k})\Pi(\mathbf{k},\mathbf{q}).\tag{12}$$

The current-operator-dependent terms $\gamma_{\alpha\beta}(\mathbf{k})$ are explicitly given as

$$\gamma_{xx}(\mathbf{k})=\{2a\sin(k_x a)[t-2t'\cos(k_y a)]\}^2,\tag{13a}$$

$$\gamma_{yy}(\mathbf{k})=\{2a\sin(k_y a)[t-2t'\cos(k_x a)]\}^2,\tag{13b}$$

$$\begin{aligned}\gamma_{xy}(\mathbf{k})=&\{2a\sin(k_x a)[t-2t'\cos(k_y a)]\}\\&\times\{2a\sin(k_y a)[t-2t'\cos(k_x a)]\}\end{aligned}\tag{13c}$$

$$=\gamma_{yx}(\mathbf{k}).\tag{13d}$$

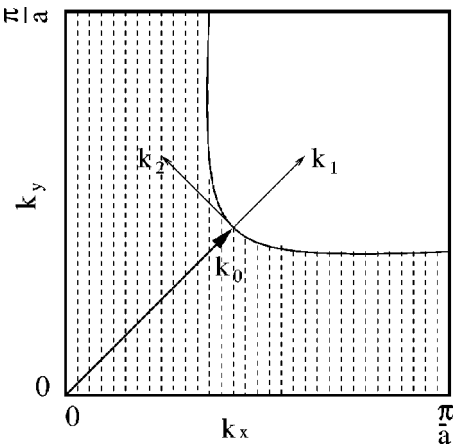

FIG. 4. New coordinate system (k_1,k_2) in the first quadrant of the atomic BZ is shown. Its origin is at the "nodal" point at which the superconducting gap vanishes on the Fermi surface. The length of the nodal vector is k_0.

The zero-frequency susceptibility of wave vector $\mathbf{q}$ for quasiparticle quasihole of momentum $\mathbf{k}$ is $\Pi(\mathbf{k},\mathbf{q})$ and has the form

$$\Pi(\mathbf{k},\mathbf{q})=\frac{1}{E_{\mathbf{k}}+E_{\mathbf{k}+\mathbf{q}}}\left[1-\frac{\xi_{\mathbf{k}}\xi_{\mathbf{k}+\mathbf{q}}+\Delta_{\mathbf{k}}\Delta_{\mathbf{k}+\mathbf{q}}}{E_{\mathbf{k}}E_{\mathbf{k}+\mathbf{q}}}\right], \tag{14}$$

with the quasiparticle energy $E_{\mathbf{k}}=\sqrt{\xi_{\mathbf{k}}^2+\Delta_{\mathbf{k}}^2}$.

It is expected that the above susceptibilities are anisotropic due to the nonlocal nature of Δ_{ij}, reflected in the $\mathbf{k}$ dependence of $\Delta_{\mathbf{k}}$. Though anisotropic, they possess certain symmetries: $\chi^{\mathrm{p}}_{\alpha\alpha}(q_x,-q_y)=\chi^{\mathrm{p}}_{\alpha\alpha}(q_x,q_y)=\chi^{\mathrm{p}}_{\alpha\alpha}(-q_x,q_y)$, $\chi^{\mathrm{p}}_{xy}(q_x,-q_y)=-\chi^{\mathrm{p}}_{xy}(q_x,q_y)=\chi^{\mathrm{p}}_{xy}(-q_x,q_y)$, and $\chi^{\mathrm{p}}_{xx}(q_x,q_y)=\chi^{\mathrm{p}}_{yy}(q_y,q_x)$. These symmetries suggest that the susceptibilities are functions of $|q_x|$, $|q_y|$, and $\mathrm{sgn}(q_xq_y)$ only. A naive perturbative expansion of $\chi^{\mathrm{p}}_{\alpha\beta}(\mathbf{q})$ in powers of q fails since the coefficient of the quadratic term in q is divergent, due to the vanishing of $\Delta_{\mathbf{k}}$ on the Fermi surface at $k_x=\pm k_y$ points. We however proceed to evaluate these analytically as follows.

We write

$$\chi^{\mathrm{p}}_{\alpha\beta}(q_x,q_y)=\sum_{j=1}^{4}\chi^{\mathrm{p},j}_{\alpha\beta}(q_x,q_y), \tag{15}$$

where $\chi^{\mathrm{p},j}_{\alpha\beta}$ is the contribution of the jth quadrant $(j=1-4)$ of k space. For instance,

$$\chi^{\mathrm{p},1}_{\alpha\beta}(q_x,q_y)=\frac{1}{(2\pi)^2}\int_0^{\pi/a}dk_x\int_0^{\pi/a}dk_y\,\gamma_{\alpha\beta}(\mathbf{k})\Pi(\mathbf{k},\mathbf{q}) \tag{16}$$

is the contribution due to the first quadrant. We present the calculation of $\chi^{\mathrm{p},1}_{\alpha\beta}(q_x,q_y)$ below in detail.

In terms of an alternative coordinate system (k_1,k_2) whose origin is at the nodal point on the Fermi surface as shown in Fig. 4, the old coordinates in the first quadrant are expressed as $k_x=(1/\sqrt{2})(k_0+k_1-k_2)$ and $k_y=(1/\sqrt{2})(k_0+k_1+k_2)$, where k_0 is defined as $\mu=-4t\cos(k_0a/\sqrt{2})+4t'\cos^2(k_0a/\sqrt{2})$. We use $\xi_{\mathbf{k}}\approx\hbar v_Fk_1$ and $\Delta_{\mathbf{k}}\approx\hbar v_\Delta k_2$ in linear form, where the Fermi velocity $v_F=(4a/\hbar\sqrt{2})[t-2t'\cos(k_0a/\sqrt{2})]\sin(k_0a/\sqrt{2})$ and $v_\Delta=(a/\hbar\sqrt{2})\Delta_0\sin(k_0a/\sqrt{2})$ is the velocity of quasiparticles along the k_2 direction. Since in d-wave superconductors $v_F\gg v_\Delta$, the phase space of k_2 effectively is much larger than that of k_1 for a given value of quasiparticle energy. We observe that this is the cause of strong anisotropy in the diagonal susceptibilities as we see below. If ϕ is the angle of a $\mathbf{k}$ vector with the k_1 axis in this new coordinate system, $\xi_{\mathbf{k}}\simeq E_{\mathbf{k}}\cos\phi$ and $\Delta_{\mathbf{k}}\simeq E_{\mathbf{k}}\sin\phi$. By Taylor expansion in q we find $\xi_{\mathbf{k}}\xi_{\mathbf{k}+\mathbf{q}}+\Delta_{\mathbf{k}}\Delta_{\mathbf{k}+\mathbf{q}}\simeq E_{\mathbf{k}}(E_{\mathbf{k}}+\alpha_{\mathbf{q}})$ and $E_{\mathbf{k}}E_{\mathbf{k}+\mathbf{q}}\simeq|E^2_{\mathbf{k}}+E_{\mathbf{k}}\alpha_{\mathbf{q}}+\beta^2_{\mathbf{q}}|$, where $\alpha_{\mathbf{q}}=\hbar(q_1v_F\cos\phi+q_2v_\Delta\sin\phi)$ and $\beta^2_{\mathbf{q}}=(\hbar^2/2)(q_1v_F\sin\phi-q_2v_\Delta\cos\phi)^2$ with $q_{1,2}=(q_y\pm q_x)/\sqrt{2}$, respectively. Since $\alpha_{\mathbf{q}}$ is negative for some region of ϕ, the quantity $(E^2_{\mathbf{k}}+E_{\mathbf{k}}\alpha_{\mathbf{q}}+\beta^2_{\mathbf{q}})$ may be negative as well as positive which we refer below as regions I and II, respectively. It is negative in the regime $E^0_1<E_{\mathbf{k}}<E^0_2$, where $E^0_1\approx(-\beta^2_{\mathbf{q}}/\alpha_{\mathbf{q}})$ and $E^0_2\approx(-\alpha_{\mathbf{q}}+\beta^2_{\mathbf{q}}/\alpha_{\mathbf{q}})$. Expanding $\gamma_{\alpha\beta}(\mathbf{k})$ up to linear order in $E_{\mathbf{k}}$, we perform the integrals over $E_{\mathbf{k}}$ in for both regions I and II separately to obtain

$$\begin{aligned}\chi^{\mathrm{p},1}_{xx}(q_x,q_y)&\approx\frac{a^2}{\pi^2\hbar^2v_Fv_\Delta}\Bigg[\int_I d\phi\Bigg\{\mathcal{R}_1[-\alpha_{\mathbf{q}}+2(\beta^2_{\mathbf{q}}/\alpha_{\mathbf{q}})\ln|\alpha_{\mathbf{q}}/\Delta_0|]\\&+\frac{2}{3}(\mathcal{D}^+_\phi\mathcal{R}_2+\mathcal{D}^-_\phi\mathcal{R}_3)(\alpha^2_{\mathbf{q}}-3\beta^2_{\mathbf{q}}-3\beta^2_{\mathbf{q}}\ln|\alpha_{\mathbf{q}}/\Delta_0|)\Bigg\}\\&+\int_{II}d\phi\{2\ln(2)(\beta^2_{\mathbf{q}}/\alpha_{\mathbf{q}})\mathcal{R}_1-2\beta^2_{\mathbf{q}}(\mathcal{D}^+_\phi\mathcal{R}_2\\&+\mathcal{D}^-_\phi\mathcal{R}_3)\ln(\alpha_{\mathbf{q}}/\Delta_0)\}\Bigg],\end{aligned} \tag{17a}$$

$$\begin{aligned}\chi^{\mathrm{p},1}_{yy}(q_x,q_y)&\approx\frac{a^2}{\pi^2\hbar^2v_Fv_\Delta}\Bigg[\int_I d\phi\Bigg\{\mathcal{R}_1[-\alpha_{\mathbf{q}}+2(\beta^2_{\mathbf{q}}/\alpha_{\mathbf{q}})\ln|\alpha_{\mathbf{q}}/\Delta_0|]\\&+\frac{2}{3}(\mathcal{D}^+_\phi\mathcal{R}_3+\mathcal{D}^-_\phi\mathcal{R}_2)(\alpha^2_{\mathbf{q}}-3\beta^2_{\mathbf{q}}-3\beta^2_{\mathbf{q}}\ln|\alpha_{\mathbf{q}}/\Delta_0|)\Bigg\}\\&+\int_{II}d\phi\{2\ln(2)(\beta^2_{\mathbf{q}}/\alpha_{\mathbf{q}})\mathcal{R}_1-2\beta^2_{\mathbf{q}}(\mathcal{D}^+_\phi\mathcal{R}_3\\&+\mathcal{D}^-_\phi\mathcal{R}_2)\ln(\alpha_{\mathbf{q}}/\Delta_0)\}\Bigg],\end{aligned} \tag{17b}$$

$$\begin{aligned}\chi^{\mathrm{p},1}_{xy}(q_x,q_y)&\approx\frac{a^2}{\pi^2\hbar^2v_Fv_\Delta}\Bigg[\int_I d\phi\Bigg\{\mathcal{R}_1[-\alpha_{\mathbf{q}}+2(\beta^2_{\mathbf{q}}/\alpha_{\mathbf{q}})\ln|\alpha_{\mathbf{q}}/\Delta_0|]\\&+\frac{2}{3}(\mathcal{R}_2+\mathcal{R}_3)\cos\phi\,(\alpha^2_{\mathbf{q}}-3\beta^2_{\mathbf{q}}-3\beta^2_{\mathbf{q}}\ln|\alpha_{\mathbf{q}}/\Delta_0|)\Bigg\}\end{aligned}$$

$$+\int_{II} d\phi\{2\ln(2)(\beta_{\mathbf{q}}^2/\alpha_{\mathbf{q}})\mathcal{R}_1 - 2\beta_{\mathbf{q}}^2(\mathcal{R}_2+\mathcal{R}_3)$$

$$\times\cos\phi\ln(\alpha_{\mathbf{q}}/\Delta_0)\}\Bigg], \tag{17c}$$

where $\mathcal{D}_\phi^{\pm}=\cos\phi\pm(v_F/v_\Delta)\sin\phi$,

$$\mathcal{R}_1=(t^2+\mu t')\sin^2(k_0a/\sqrt{2}), \tag{18a}$$

$$\mathcal{R}_2=2\sqrt{2}\left(\frac{a}{\hbar v_F}\right)t'[t-2t'\cos(k_0a/\sqrt{2})]\sin^3(k_0a/\sqrt{2}), \tag{18b}$$

$$\mathcal{R}_3=\sqrt{2}\left(\frac{a}{\hbar v_F}\right)(t^2+\mu t')\sin(k_0a/\sqrt{2})\cos(k_0a/\sqrt{2}), \tag{18c}$$

and $\int_I$ and $\int_{II}$ represent the integrals over ϕ $(0\leqslant\phi\leqslant 2\pi)$ for the regime of ϕ in which $\alpha_{\mathbf{q}}<0$ and >0, respectively. We, similarly, calculate $\chi_{\alpha\beta}^{\mathrm{p},j}$ for three other quadrants. We observe that $\chi_{xx}^{\mathrm{p},1}$ and $\chi_{yy}^{\mathrm{p},1}$ differ substantially through the last terms within both the integrals $\int_I$ and $\int_{II}$ in their expressions (17a) and (17b) since $v_F\gg v_\Delta$. These lead to an anisotropic diagonal susceptibility. We note that these terms—also the terms involving $\int_{II}$—arise due to keeping the linear dependences of k_1 and k_2 in $\gamma_{\alpha\beta}(\mathbf{k})$. However, for an approximation $k_x=k_y=k_0/\sqrt{2}$ in $\gamma_{\alpha\beta}(\mathbf{k})$, $\chi_{xx}^{\mathrm{p}}=\chi_{yy}^{\mathrm{p}}$ as obtained by Franz *et al.*[12]

Since the angular integrals in the expressions for $\chi_{\alpha\beta}^{\mathrm{p}}$ cannot be performed analytically, we numerically integrate these to obtain $\chi_{\alpha\beta}^{\mathrm{p}}$ in the next section. We shall then compare these semianalytically obtained $\chi_{\alpha\beta}^{\mathrm{p}}$ with those completely numerically obtained through Eqs. (12)–(14).

We now turn to obtain the equation for the vector potential in the gauge $\mathbf{G}\cdot\mathbf{A}_{\mathbf{G}}=0$ [from Eq. (11)]. By minimizing the energy with respect to as $\mathbf{A}_{\mathbf{G}}$, we have

$$(A_{\mathbf{G}})_\alpha=\frac{4\pi e}{\hbar cG^2d}[\chi^d\delta_{\alpha\beta}-\chi_{\alpha\beta}^{\mathrm{p}}(\mathbf{G})]\left[\frac{1}{2}(\nabla\theta)_{-\mathbf{G}}-\frac{e}{\hbar c}A_{-\mathbf{G}}\right]_\beta. \tag{19}$$

We thus obtain

$$\left[\frac{\hbar}{2}(\nabla\theta)_{-\mathbf{G}}\right]_\alpha=[G^2Q_{\beta\alpha}^{-1}+\delta_{\beta\alpha}]\left(\frac{e}{c}A_{-\mathbf{G}}\right)_\beta, \tag{20}$$

where

$$Q_{\alpha\beta}(\mathbf{q})=\frac{1}{\lambda^2}\delta_{\alpha\beta}-\left(\frac{4\pi e^2}{c^2\hbar^2d}\right)\chi_{\alpha\beta}^{\mathrm{p}}(\mathbf{q}). \tag{21}$$

Using Eq. (20) in Eq. (11), we get

$$\Delta\Omega=\frac{1}{8\pi A}\sum_{\mathbf{G}} B_{\mathbf{G}}\left[1+\frac{G_\alpha Q_{\alpha\beta}G_\beta}{\mathrm{Det}\,Q}\right]B_{-\mathbf{G}}. \tag{22}$$

We now express $B_{\mathbf{G}}$ in terms of $N_v,\Phi_0,Q_{\alpha\beta}$, and $\mathbf{G}$. For a vortex lattice,

$$(\boldsymbol{\nabla}\theta)_{\mathbf{G}}=2i\pi N_v\frac{\mathbf{G}\times\hat{e}_z}{G^2}, \tag{23}$$

where N_v is the total number of vortices. We then obtain from Eqs. (19) and (20)

$$B_{\mathbf{G}}=N_v\Phi_0\left[\frac{\mathrm{Det}\,Q+Q_{\alpha\beta}\epsilon^{\alpha\gamma}\epsilon^{\beta\delta}G_\gamma G_\delta}{G^4+G^2Q_{\alpha\beta}\delta_{\alpha\beta}+\mathrm{Det}\,Q}\right], \tag{24}$$

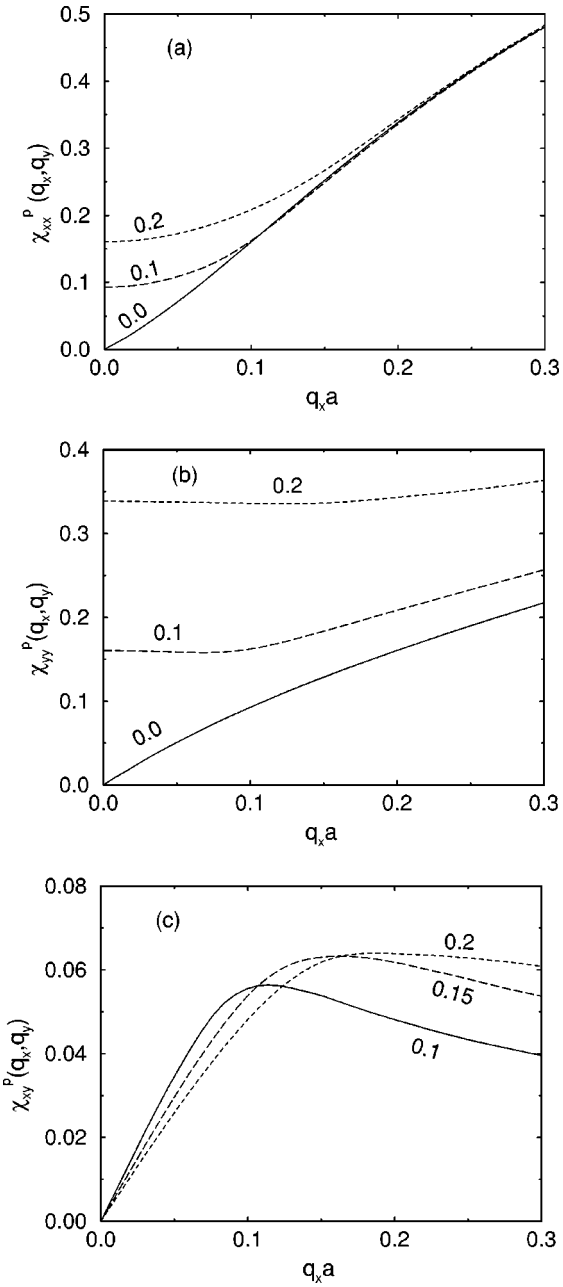

FIG. 5. Dimensionless susceptibilities (a) χ_{xx}^{p}, (b) χ_{yy}^{p}, and (c) χ_{xy}^{p} (in units of χ_d) plotted against small positive q_xa. The numbers associated with each curve are the corresponding values of q_ya. The susceptibilities for negative values of q_x and q_y are related to the same for positive values of q_x and q_y by the symmetries discussed in the text.

with $\epsilon^{12}=1=-\epsilon^{21}$, $\epsilon^{11}=0=\epsilon^{22}$, and $\Phi_0=hc/2e$ is the quantum of flux. Therefore, the free energy for a vortex lattice per unit volume becomes

$$\mathcal{F}=\frac{1}{8\pi}(\Phi_0 n_v)^2\sum_{\mathbf{G}}\left[\frac{\mathrm{Det}\,Q+Q_{\alpha\beta}\epsilon^{\alpha\gamma}\epsilon^{\beta\delta}G_\gamma G_\delta}{G^4+G^2Q_{\alpha\beta}\delta_{\alpha\beta}+\mathrm{Det}\,Q}\right]^2 \times\left[1+\frac{G_\alpha Q_{\alpha\beta}G_\beta}{\mathrm{Det}\,Q}\right]. \tag{25}$$

This has an approximate but much simpler form as

$$\mathcal{F}\simeq\frac{1}{8\pi}(\Phi_0 n_v)^2\sum_{\mathbf{G}}\frac{G_x^2Q_{yy}+G_y^2Q_{xx}-G_xG_y(Q_{xy}+Q_{yx})}{G^4}, \tag{26}$$

which is essentially important for determining the ground-state structure of the vortex lattice. This form is exact when $|(\hbar/2)(\nabla\theta)_{\mathbf{G}}|\geqslant|eA_{\mathbf{G}}|/c$ which is true. The component $G=0$ will give free energy $\overline{\mathcal{F}}$ for average magnetic induction B. For determination of the vortex lattice structure, one should in principle minimize the Gibbs free energy $\mathcal{G}=\mathcal{F}-BH/4\pi$. Here H is the applied magnetic field. Beyond H_{c_1}, the magnetic field penetrates the superconductor almost fully. Thus $B\simeq H$, especially so in high-T_c superconductors, since $H_{c_1}\ll H_{c_2}$. Here B does not vary much for different vortex lattice structures for a given H as we see in our numerical study that the ratio $(H-B)/B\sim10^{-7}$. We therefore minimize $\Delta\mathcal{F}=\mathcal{F}-\overline{\mathcal{F}}$, i.e., that part of the free energy which depends on G, in Eq. (26), for different choices of nonzero G's corresponding to different structures and with a cutoff $G\leqslant\pi/\xi$.

III. NUMERICAL STUDY

The values of the phenomenological parameters that we have used for the numerical computation of $Q_{\alpha\beta}(q_x,q_y)$ and later for the free energy are taken from angle-resolved photoemission experiments,[16,18] penetration depth measurement,[24] and band structure calculations[25] for high-T_c compounds. These are as follows: $t=1150$ K, $t'=0.48t$, $\Delta_0=400$ K, $a=3.8$ Å, $d=10$ Å, $\xi=20$ Å, $\lambda=1600$ Å, and $\mu=-1.33t$ which corresponds to doping concentration $x\simeq0.19$.

Using standard Gaussian quadrature, we integrate over k_x and k_y in Eq. (12) to obtain $\chi^{\mathrm{p}}_{\alpha\beta}(\mathbf{q})$. In Fig. 5 we show the dependence of paramagnetic susceptibilities (a) χ^{p}_{xx}, (b) χ^{p}_{yy}, and (c) χ^{p}_{xy} in units of χ^d for positive q_x at different positive values of q_y. Susceptibilities for negative values of q_x and q_y can be obtained by using the symmetries discussed in the previous section. We see that $\chi^{\mathrm{p}}_{xx}(q_x,q_y)\neq\chi^{\mathrm{p}}_{yy}(q_x,q_y)$ in general. This strong anisotropy in the diagonal susceptibilities is due to the strong $\mathbf{k}$ dependence of the nature of $\Delta_{\mathbf{k}}$ and the $\mathbf{k}$-dependent $\gamma_{\alpha\beta}(\mathbf{k})$, Eqs. (13a)–(13d). The diagonal susceptibilities are large compared to the off-diagonal one.

We numerically fit, guided by the semianalytical form in Eqs. (17a)–(17c), to obtain the approximate functional form of $\chi^{\mathrm{p}}_{\alpha\beta}(q_x,q_y)$ for $q_xa,q_ya\leqslant0.3$ as

$$\chi^{\mathrm{p}}_{xx}(q_x,q_y)=\begin{cases}\gamma\,[0.31(\delta|q_x|a)+0.14(\delta q_xa)^2-0.35(\delta q_xa)^2\ln|\delta q_xa|] & \text{if}\quad |q_x|\geqslant|q_y|,\\ \gamma\left[0.35(\delta|q_y|a)-0.14(\delta q_ya)^2+0.10(\delta q_ya)^2\ln|\delta q_ya|\right.\\ \left.+\left(0.10+\dfrac{0.21}{\delta|q_y|a}\right)(\delta q_xa)^2+\left(-0.16+\dfrac{0.07}{\delta|q_y|a}\right)(\delta q_xa)^2\ln|\delta q_xa|\right] & \text{if}\quad |q_x|\leqslant|q_y|,\end{cases} \tag{27a}$$

$$\chi^{\mathrm{p}}_{yy}(q_x,q_y)=\chi^{\mathrm{p}}_{xx}(q_y,q_x), \tag{27b}$$

$$\chi^{\mathrm{p}}_{xy}(q_x,q_y)=\gamma\left[\left(0.11+\frac{0.02}{q_>}\right)q_<+\left(0.15-\frac{0.18}{q_>}\right)q_<^2+\left(0.07-\frac{0.12}{q_>}\right)q_<^2\ln q_<\right]\mathrm{sgn}(q_xq_y), \tag{27c}$$

with $q_{>,<}=\max,\min(|q_x|,|q_y|)\,\delta a$, $\gamma=(\lambda^2/d)\times(4\pi e^2/c^2\hbar^2)t$ whose numerical value is 1.18, and the parameter $\delta=t/\Delta_0$. These phenomenological forms can be explained from the semianalytical expressions (17a)–(17c) as follows. (i) First, why do $\chi^{\mathrm{p}}_{xx}(q_x,q_y)$ and $\chi^{\mathrm{p}}_{yy}(q_x,q_y)$ not depend on the signs of q_x and q_y, and $\chi^{\mathrm{p}}_{xy}(q_x,q_y)$ does depend on $\mathrm{sgn}(q_xq_y)$? This is due to the symmetry reason discussed following Eq. (14). (ii) Why does $\chi^{\mathrm{p}}_{xx}(q_x,q_y)$ mainly depend on whether $|q_x|\geqslant|q_y|$ or not? This can be understood by the following exercise. We find a term from Eq. (17a) as $|q_y+q_x|$ assuming $q_x,q_y\geqslant0$. The corresponding term will be $|q_y-q_x|$ when we consider the contribution from the second quadrant. When we add these two contributions, we see that the sum depends on the greater of q_x and q_y. (iii) Following the argument above in (ii), the difference between the two terms is the smaller of q_x and q_y. This is the reason why $\chi^{\mathrm{p}}_{xy}(q_x,q_y)$ depends mainly on the smaller of $|q_x|$ and $|q_y|$. (iv) Since $\chi^{\mathrm{p},1}_{xx}(q_x,q_y)\neq\chi^{\mathrm{p},1}_{yy}(q_x,q_y)$ and $\chi^{\mathrm{p}}_{xx}(q_x,q_y)=\chi^{\mathrm{p}}_{yy}(q_y,q_x)$ for symmetry reasons, the dependence of $\chi^{\mathrm{p}}_{xx}(q_x,q_y)$ on q_x and q_y is asymmetric. (v) The linear, quadratic, and the logarithmic dependences on q follow from in the expressions (17a)–(17c).

We next numerically perform angular integrals in Eqs. (17a)–(18c) along with the contributions from other three

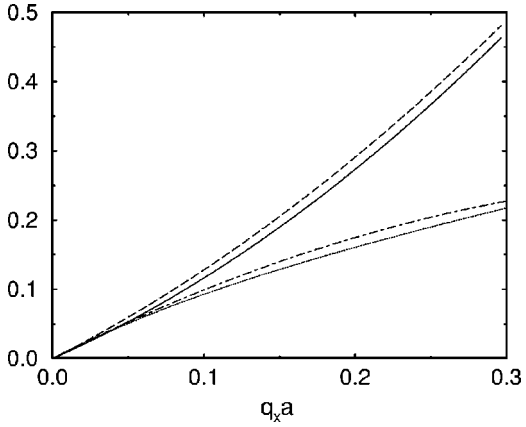

FIG. 6. Numerically (dashed and dotted lines) and semianalytically (solid and dot-dashed lines) obtained $\chi^{\rm p}_{xx}(q_x,0)$ and $\chi^{\rm p}_{yy}(q_x,0)$ (in units of χ_d), respectively.

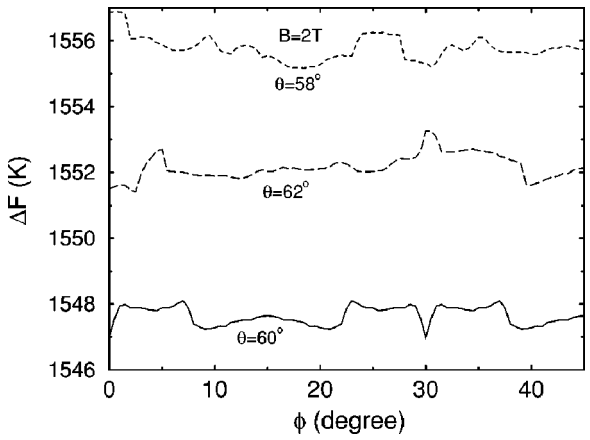

FIG. 7. Free energy per vortex as a function of ϕ for $\theta=58°$, 60°, and 62° at 2 T field.

quadrants to obtain semianalytical susceptibilities and then compare with the fully numerically obtained susceptibilities. In Fig. 6 we show $\chi^{\rm p}_{xx}(q_x,0)$ and $\chi^{\rm p}_{yy}(q_x,0)$ evaluated in the two ways. The linear approximation of energies in the analytical expressions is a good approximation for determining linear dependence on q_x as we see in Fig. 6 that they agree for very low q_x. They however differ for higher q_x since our analytical expressions are not consistent in determining quadratic dependences on q as we have neglected higher-order k dependences to the quasiparticle energy. It is, however, clear that $\chi^{\rm p}_{xx}\neq\chi^{\rm p}_{yy}$ which is our main result.

We consider a face-centered rectangular vortex lattice (as shown in Fig. 2) with area of the unit cell, $\tilde{A}=2\Phi_0/B$, in general. The angle θ determines the sides of the rectangle with a fixed area. The sides of the rectangle are $a_1=[\tilde{A}\tan\theta]^{1/2}$ and $a_2=[\tilde{A}/\tan\theta]^{1/2}$. We then readily obtain reciprocal lattice vectors for a vortex lattice, in general, to be

$$G_{mn}(B,\theta)=(n+m)\frac{2\pi}{a_1}\hat{e}_x+(n-m)\frac{2\pi}{a_2}\hat{e}_y, \qquad (28)$$

where n and m are integers (both positive and negative) including zero. If the vortex lattice makes an angle ϕ with the underlying atomic lattice, we find

$$G_{mn}(B,\theta,\phi)=\hat{e}_x\left[(n+m)\frac{2\pi}{a_1}\cos\phi-(n-m)\frac{2\pi}{a_2}\sin\phi\right] +\hat{e}_y\left[(n+m)\frac{2\pi}{a_1}\sin\phi+(n-m)\frac{2\pi}{a_2}\cos\phi\right]. \qquad (29)$$

The lattice is a centered square for $\theta=45°$ and triangular when $\theta=60°$. There is symmetry of rotation about $\phi=45°$, since the lattice is considered as centered rectangular. We therefore need to determine free energy for $45°\leqslant\theta<90°$ and $0\leqslant\phi\leqslant45°$.

We then numerically compute the free energy per vortex (without the single-vortex energy which does not depend on structure), $\Delta F=d\Delta\mathcal{F}/n_v$, using Eqs. (26) and (29) as functions of the parameters θ, ϕ, and B. The reciprocal lattice vector $\mathbf{G}$ changes with the change of any one or more of the parameters. Thus ΔF differs for different combination of these parameters (ϕ,θ,H). In Fig. 7 we show the dependence of ΔF at a low field $B=2$ T as a function of ϕ for the angles $\theta=60°$ and two neighboring angles $\theta=58°$ and 62° (on either side of $\theta=60°$). It is clear that ΔF is a minimum for the triangular lattice. We notice also that ΔF is a minimum for the triangular lattice when $\phi=0°$ and 30°, which in fact correspond to the same lattice configuration. We likewise find that in the whole of the low-field regime, the ground-state configuration of the vortex lattice is triangular with one of its arms parallel to one of the crystal axes.

Interestingly, the orientation of the lattice changes discontinuously as we increase the magnetic field though the structure continues to be triangular. In Fig. 8 we show the dependence of ΔF on ϕ for the triangular lattice configuration at three chosen fields 2, 5, and 8 T. At nearly about 5 T field, ΔF is minimum for all 0°, 30°, 15°, and 45° orientations; the latter two angles correspond to the same lattice configuration, like the former two angles. On the other hand, at the field of 8 T, ΔF is minimum for $\phi=15°$ and 45° only. The triangular vortex lattice changes its orientation discontinuously at about 5 T field. While the triangular lattice has one of its arms parallel to one of the crystal axes at lower field; it aligns to one of the crystal axes by 45° at higher field. We understand this discontinuous transition by comparing the energies contributed to ΔF by the $\mathbf{G}$ vectors of the lowest magnitude (since they contribute most to the free energy) for these two preferred orientations. Considering the symmetries of the susceptibilities, it is sufficient that we consider only those $\mathbf{G}$ vectors which have positive G_x. We thus consider three $\mathbf{G}$ vectors for each of these two orientations. These are (a) $(1/2,\pm\sqrt{3}/2)G$ and $(1,0)G$ for $\phi=0°$ and (b) $(1/2\sqrt{2})\times(\sqrt{3}-1,\sqrt{3}+1)G$, $(1/2\sqrt{2})(\sqrt{3}+1,\sqrt{3}-1)G$, and $(1/\sqrt{2},1/\sqrt{2})G$ for $\phi=45°$, where the length of the smallest $\mathbf{G}$ vector $G=2\pi(2/\sqrt{3})^{1/2}(B/\Phi_0)^{1/2}$. In Fig. 9, we show the energy E contributed by these individual $\mathbf{G}$ vectors to ΔF for 2, 5, and 8 T fields. We find the total energy contributed by the above three $\mathbf{G}$ vectors for $\phi=0°$ and 45° orientations as (a) 296.05 K and 296.51 K for $B=2$ T, (b) 282.96 K and

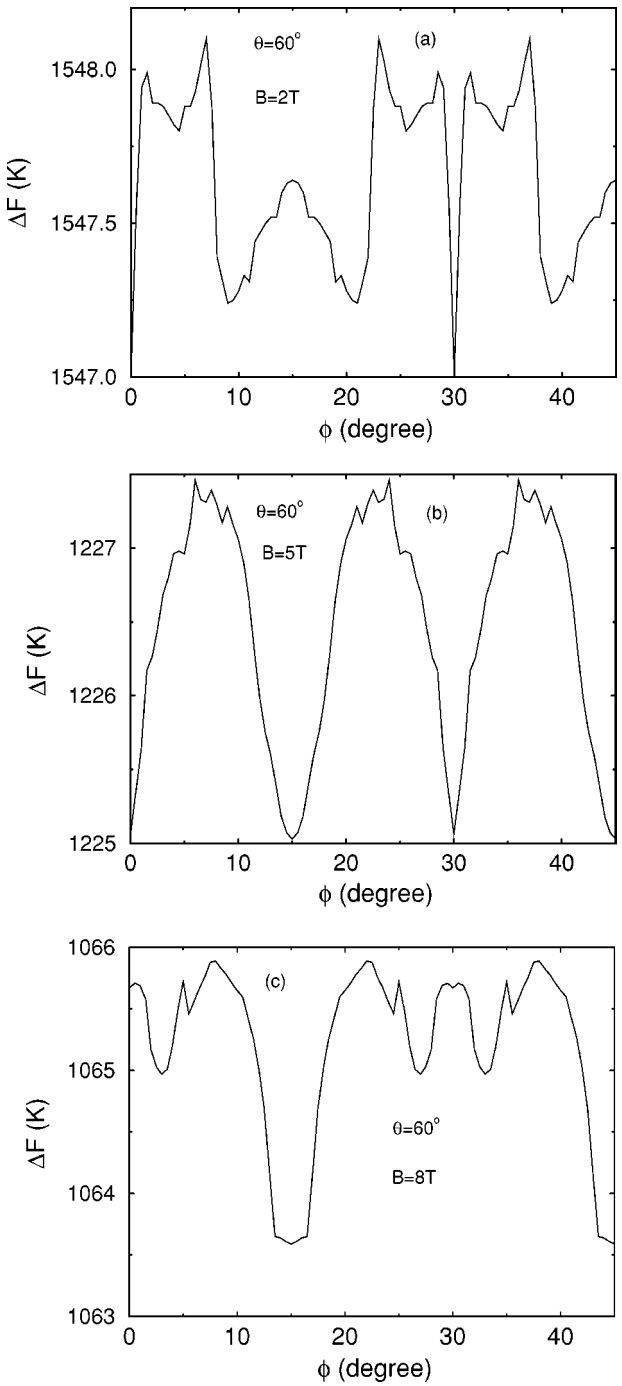

FIG. 8. Free energy per vortex for triangular lattice structure ($\theta=60°$) as a function of its orientation angles ϕ for (a) $B=2$ T, (b) $B=5$ T, and (c) $B=8$ T fields.

283.11 K for $B=5$ T, and (c) 274.15 K and 273.60 K for $B=8$ T, respectively. Clearly, the triangular lattice makes an orientational transition at about the 5 T field.

To understand the field scale 5 T for the above orientational transition, we compare the energy contributed by the above three **G** vectors for each of the preferred orientations. The ratio of these energies can be expressed as a function of $\alpha=tGa/\Delta_0$ using Eqs. (26)–(29). This is given by

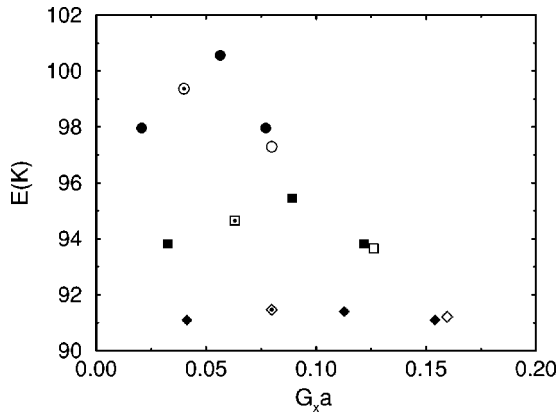

FIG. 9. The contributions to the energy per vortex by the three lowest **G** vectors of equal length for positive G_x at three different fields for two different commensurate orientations of the triangular lattice. The open (solid) symbols represent 0° (45°) orientation of the vortex lattice with respect to crystalline lattice. The open symbols with a dot in their centers correspond to the energy for two different **G** vectors with same G_x. The circles, squares, and diamonds correspond to 2, 5, and 8 T fields, respectively.

$$\frac{E_1}{E_2}=\frac{3-f_1(\alpha)}{3-f_2(\alpha)}, \tag{30}$$

where E_1 (E_2) is the energy contributed by the above corresponding three **G** vectors of triangular lattice with 0° (45°) orientation. In Fig. 10, we show the ratio $f_1(\alpha)/f_2(\alpha)$ as a function of α. The orientational transition takes place when the ratio is unity. This corresponds to $\alpha_c=tG_ca/\Delta_0\simeq 0.37$. Therefore the critical field at which the transition takes place, $B_1\simeq(0.37/2\sqrt{2}\pi)^2\sqrt{3}(\Delta_0/at)^2\Phi_0\simeq 5.2$ T.

The structure of the vortex lattice remains triangular with 45° orientation to the crystal lattice as shown ΔF in Fig. 11 for a field as high as 25 T. However, it makes yet another discontinuous structural transition to a centered square lattice with its axes parallel to the crystal axes at yet another critical field B_2 whose value is about 28 T. Figure 12 shows that ΔF is minimum for $\theta=45°$ and $\phi=0°$ at $B=28$ T. The overall

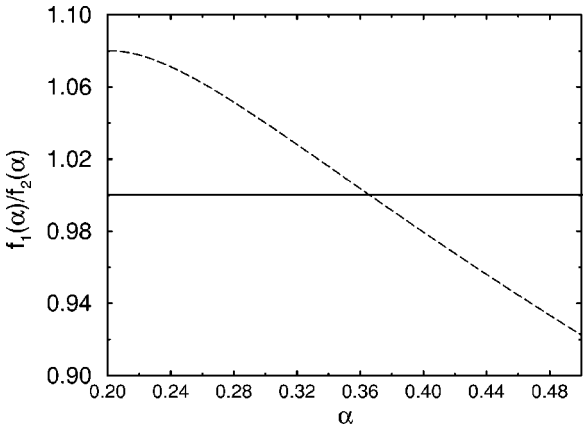

FIG. 10. The dashed line represents the ratio $f_1(\alpha)/f_2(\alpha)$ as a function of α. The solid line is a guide to the eyes for the value of the ratio 1.0.

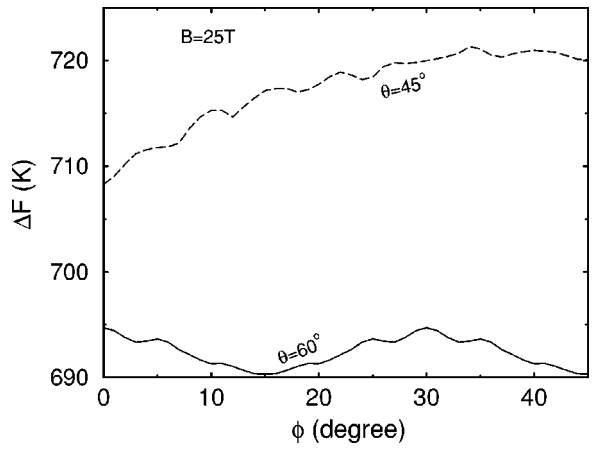

FIG. 11. Free energy per vortex as a function of ϕ for $\theta=60°$ and 45° at a high field $B=25$ T.

phase diagram for the ground state of the vortex lattice structure at $T=0$ is shown in Fig. 1.

IV. CONCLUDING REMARKS

We conclude by briefly discussing a number of questions such as the nature of the approximations used, the effect of nonzero temperature, consequences of the transitions, their observability, the reason why our conclusions differ from those found earlier, and the structural transitions experimentally observed.

We have calculated the ground-state energy assuming effectively that the interaction between two vortices is unaffected by the presence of other vortices. This is obviously a low-vortex-density approximation which seems quite reasonable since the dimensionless ratio (n_v/n) is about 1/2500 for a field of 1 T. However, we have not calculated the higher-order corrections which while nominally of higher order in (n_v/n) might have large or even divergent coefficients. Since the vortex interaction depends on the quasiparticle-quasihole susceptibility, a change in their spectrum due to the supercurrent (the Volovik effect[26]) could have serious consequences. Here, we would like to make two points. First, a calculation by Amin, Affleck, and Franz,[13] using a semiclassical approximation to include the nonlinear effect of the magnetic field in the manner of Volovik, finds that this has little effect on the structural transformations calculated by them. Second, *all* the recent fully quantum mechanical calculations[27,28] of the density of Dirac quasiparticle states in a vortex lattice in the London limit find that for Bravais lattices the density of states vanishes linearly with energy as in the absence of a magnetic field; only the slope changes. A general argument for this has been presented by Vishwanath.[29] For these two reasons, we believe that our low-density approximation is reliable.

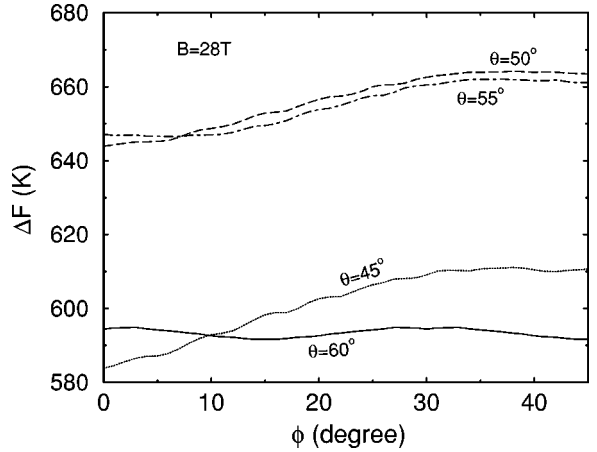

FIG. 12. Free energy per vortex as a function of ϕ for $\theta=45°$, 50°, 55°, and 60° at $B=28$ T field. Clearly ΔF is minimum for the structure corresponding to $\theta=45°$ and $\phi=0°$.

In the London approximation, the vortex cores are treated as δ functions. In reality, they have a width of the order of the coherence length. We believe that the consequences of this approximation, at least for the low-field structural transition, are small. The reason is that the structure-sensitive part of the energy arises from the difference in the contribution of the smallest reciprocal lattice vectors (Sec. III). For these, $G\xi\sim(1/10)$ at typical magnetic fields, so that the phenomenological assumption of a Gaussian vortex core with width $\sim\xi$ will make a negligible difference to the structure-sensitive part.

We have calculated only the ground-state energy of the vortex lattice in this paper. At any nonzero temperature, there are obviously entropic contributions which could change the magnetic field at which the structural transition occurs, as a function of temperature. Here, we note that since both the structures (below and above 5 T) are identical (triangular) and the structure difference sensitive part of the energy is a tiny fraction $[<(1/1000)^2]$ of the vortex interaction energy, the elastic fluctuations in both structures are expected to be identical to order $(1/1000)^2$ so that the transition field should not be affected by temperature, as long as the input parameters (e.g., $\xi_{\mathbf{k}},\Delta_{\mathbf{k}},\lambda$) do not change with T. The same cannot be said of the high-field ($\sim$28 T) triangular to centered square lattice transition, because one has a tight-packed structure and the other not. The expectation is that the former has fewer elastic fluctuations than the latter, so that the transition field boundary should shift to lower values with increasing temperature. However, this conclusion is tempered by the fact that the London approximation is unreliable at these high fields when vortex cores get close to each other so that our basic result may not be that reliable.

One interesting consequence of the orientational transition at 5 T, which might be measurable, is the change in the very low energy density of quasiparticle states. At least for a square lattice, Vishwanath[29] has shown that there are quasiparticle states with linear dispersion and that there is a very small gap arising from higher-order terms in the quasiparticle velocity. If this kind of result carries through for a triangular lattice, then it might be an experimental way of observing the transition.

We have calculated here the actual energy of the structure-sensitive term (Sec. III) and have found it to be small, of the order of a few degrees per vortex. Because of this reason, the transition might be difficult to observe, since pinning energies of larger size are generally present,[30] unless

the system is extremely perfect.

We have discussed in detail (Sec. II and III) the reason why our results differ from those obtained earlier. Basically, it has to do with the anisotropy of the nonlocal current susceptibility, i.e., the fact that $\chi^{p}_{xx}(\mathbf{G}) \neq \chi^{p}_{yy}(\mathbf{G})$. The reason for this essentially is that we have an anisotropic superconductor. The χ^{p}_{xx} and χ^{p}_{yy} functions are plotted in Fig. 5.

The question of a nontriangular structure of the vortex lattice in cuprates has attracted considerable experimental attention,[6–8] especially since it has become established that they are $d_{x^2-y^2}$ superconductors. Earlier small-angle neutron scattering measurements[7] were on highly twinned 123 crystals, so that the observation of fourfold diffraction symmetry does not imply a rectanglar or square lattice. Moreover, the positional order is very poor. A more recent experiment[8] on untwinned 123 single crystals shows much better translational order (higher G peaks are resolved) and a triangular lattice with axes oriented along a, distorted because of a-b asymmetry. The authors find no structural transitions up to 4 T with field along the c axis. They however find a transition from a triangular lattice oriented along a to one oriented along the b axis at a field of about 3.8 T, oriented at 33° to the c axis. This is certainly quite different from the transition to a triangular lattice at 45° to the a axis at 5 T predicted by us. As Johnson *et al.* point out[8] the observed transition could be due to the presence of chains in 123 and the novel ab-c anisotropy caused by it (which may have a strong effect on many physical properties). In order to seriously explore our conclusions, one needs to do experiments on cuprates without chains and ideally with tetragonal symmetry, as again mentioned by Johnson *et al.*[8]

ACKNOWLEDGMENTS

One of us (T.V.R.) acknowledges support from the JNC India and the U.S.-India ONR funded Project No. N00014-97-0988.

*Also at Condensed Matter Theory Unit, Jawaharlal Nehru Centre for Advanced Scientific Research, Jakkur, Bangalore 560 064, India.

†Present address: Department of Physics, 104 Davey Laboratory, The Pennsylvania State University, University Park, PA 16802.

[1] A. A. Abrikosov, Sov. Phys. JETP **5**, 1174 (1957).

[2] U. Essmann and H. Trauble, Phys. Lett. **24A**, 526 (1967).

[3] H. F. Hess, R. B. Robinson, R. C. Dynes, J. M. Valles, Jr., and J. V. Waszczak, Phys. Rev. Lett. **62**, 214 (1989).

[4] R. N. Kleiman, C. Broholm, G. Aeppli, E. Bucher, N. Stucheli, D. J. Bishop, K. N. Clausen, K. Mortensen, J. S. Pedersen, and B. Howard, Phys. Rev. Lett. **69**, 3120 (1992).

[5] T. M. Riseman, P. G. Kealey, E. M. Forgan, A. P. Mackenzie, L. M. Galvin, A. W. Tyler, S. L. Lee, C. Ager, D. McK. Paul, C. M. Aegerter, R. Cubitt, Z. Q. Mao, T. Akima, and Y. Maeno, Nature (London) **396**, 242 (1998); P. G. Kealey, T. M. Riseman, E. M. Forgan, L. M. Galvin, A. P. Mackenzie, S. L. Lee, D. McK. Paul, R. Cubitt, D. F. Agterberg, R. Heeb, Z. Q. Mao, and Y. Maeno, Phys. Rev. Lett. **84**, 6094 (2000).

[6] I. Maggio-Aprile, Ch. Renner, A. Erb, E. Walker, and Ø. Fischer, Phys. Rev. Lett. **75**, 2754 (1995).

[7] B. Keimer, W. Y. Shih, R. W. Erwin, J. W. Lynn, F. Dogan, and I. A. Aksay, Phys. Rev. Lett. **73**, 3459 (1994).

[8] S. T. Johnson, E. M. Forgan, S. H. Lloyd, C. M. Aegerter, S. L. Lee, R. Cubitt, P. G. Kealey, C. Ager, S. Tajima, A. Rykov, and D. McK. Paul, Phys. Rev. Lett. **82**, 2792 (1999).

[9] M. Ichioka, N. Hayashi, N. Enomoto, and K. Machida, Phys. Rev. B **53**, 15 316 (1996).

[10] H. Won and K. Maki, Phys. Rev. B **53**, 5927 (1996).

[11] I. Affleck, M. Franz, and M. H. S. Amin, Phys. Rev. B **55**, R704 (1997).

[12] M. Franz, I. Affleck, and M. H. S. Amin, Phys. Rev. Lett. **79**, 1555 (1997).

[13] M. H. S. Amin, I. Affleck, and M. Franz, Phys. Rev. B **58**, 5848 (1998).

[14] G. Blatter, M. V. Feigel'man, V. B. Geshkenbein, A. I. Larkin, and V. M. Vinokur, Rev. Mod. Phys. **66**, 1125 (1994); A. Schilling, R. A. Fisher, N. E. Phillips, U. Welp, D. Dasgupta, W. K. Kwok, and G. W. Crabtree, Nature (London) **382**, 791 (1996); R. J. Drost, C. J. van der Beek, J. A. Heijn, M. Konczykowski, and P. H. Kes, Phys. Rev. B **58**, R615 (1998); S. L. Lee, C. M. Aegerter, S. H. Lloyd, E. M. Forgan, C. Ager, M. B. Hunt, H. Keller, I. M. Savic, R. Cubitt, G. Wirth, K. Kadowaki, and N. Koshizuka, Phys. Rev. Lett. **81**, 5209 (1998); M. J. W. Dodgson, V. B. Geshkenbein, and G. Blatter, *ibid.* **83**, 5358 (1999); C. J. van der Beek, M. Konczykowski, R. J. Drost, P. H. Kes, N. Chikumoto, and S. Bouffard, Phys. Rev. B **61**, 4259 (2000); M. Muller, D. A. Gorokhov, and G. Blatter, *ibid.* **64**, 134523 (2001).

[15] W. N. Hardy, D. A. Bonn, D. C. Morgan, R. Liang, and K. Zhang, Phys. Rev. Lett. **70**, 3999 (1993); D. A. Wollman, D. J. van Harlingen, W. C. Lee, D. M. Ginsberg, and A. J. Leggett, *ibid.* **71**, 2134 (1993); C. C. Tsuei, J. R. Kirtley, C. C. Chi, L. S. Yu-Jajnes, A. Gupta, T. Shaw, J. Z. Sun, and M. B. Ketchen, *ibid.* **73**, 593 (1994).

[16] H. Ding, M. R. Norman, J. C. Campuzano, M. Randeria, A. F. Bellman, T. Yokoya, T. Takahasi, T. Mochiku, and K. Kadowaki, Phys. Rev. B **54**, R9678 (1996).

[17] D. A. Bonn, P. Dosanjh, R. Liang, and W. N. Hardy, Phys. Rev. Lett. **68**, 2390 (1992); K. Krishana, J. M. Harris, and N. P. Ong, *ibid.* **75**, 3529 (1995); K. Krishana, N. P. Ong, Y. Zhang, Z. A. Xu, R. Gagnon, and L. Taillefer, *ibid.* **82**, 5108 (1999); A. Hosseini, R. Harris, S. Kamal, P. Dosanih, J. Preston, R. Liang, W. N. Hardy, and D. A. Bonn, Phys. Rev. B **60**, 1349 (1999).

[18] M. R. Norman, M. Randeria, H. Ding, and J. C. Campuzano, Phys. Rev. B **52**, 615 (1995).

[19] K. A. Moler, D. J. Baar, J. S. Urbach, R. Liang, W. N. Hardy, and A. Kapitulnik, Phys. Rev. Lett. **73**, 2744 (1994); B. Revaz, J.-Y. Genoud, A. Junod, K. Neumaier, A. Erb, and E. Walker, *ibid.* **80**, 3364 (1998); D. A. Wright, J. P. Emerson, B. F. Woodfield, J. E. Gordon, R. A. Fisher, and N. E. Phillips, *ibid.* **82**, 1550 (1999).

[20] K. Krishana, N. P. Ong, Q. Li, G. D. Gu, and N. Koshizuka, Science **277**, 83 (1997); H. Aubin, K. Behnia, S. Ooi, and T. Tamegai, Phys. Rev. Lett. **82**, 624 (1999); B. Zeini, A. Freimuth, B. Buchner, R. Gross, A. P. Kampf, M. Klaser, and H. M. -Vogt, *ibid.* **82**, 2175 (1999); M. Chiao, R. W. Hill, C. Lupien, B. PopiC, R. Gagnon, and L. Taillefer, *ibid.* **82**, 2943 (1999); N. P. Ong, K. Krishana, Y. Zhang, and Z. A. Xu, in *Physics and Chemistry of Transition Metal Oxides*, edited by H. Fukuyama

and N. Nagaosa (Springer-Verlag, Berlin, 1999), p. 202; Y. Ando, J. Takeya, Y. Abe, K. Nakamura, and A. Kapitulnik, Phys. Rev. B **62**, 626 (2000).
[21] J. E. Sonier, J. H. Brewer, R. E. Kiefl, G. D. Morris, D. A. Bonn, J. Chakhalian, R. H. Heffner, W. N. Hardy, and R. Liang, Phys. Rev. Lett. **83**, 4156 (1999).
[22] I. Kosztin and A. J. Leggett, Phys. Rev. Lett. **79**, 135 (1997).
[23] A. Paramekanti, M. Randeria, T. V. Ramakrishnan, and S. S. Mandal, Phys. Rev. B **62**, 6786 (2000).
[24] S. Kamal, R. Liang, A. Hosseini, D. A. Bonn, and W. N. Hardy, Phys. Rev. B **58**, R8933 (1998).
[25] E. Dagotto, Rev. Mod. Phys. **66**, 763 (1994).
[26] G. E. Volovik, JETP Lett. **58**, 469 (1993).
[27] M. Franz and Z. Tesanovic, Phys. Rev. Lett. **84**, 554 (2000); O. Vafek, A. Melikyan, M. Franz, and Z. Tesanovic, Phys. Rev. B **63**, 134509 (2001).
[28] L. Marinelli, B. I. Halperin, and S. H. Simon, Phys. Rev. B **62**, 3488 (2000).
[29] A. Vishwanath, cond-mat/0104213 (unpublished).
[30] See, for example, C. Attanasio, L. Maritato, C. Coccorese, S. L. Prischepa, A. N. Lykov, and M. Salvato, IEEE Trans. Appl. Supercond. **5**, 1359 (1995).